JOURNAL OF BONE AND MINERAL RESEARCH
Volume 23, Number 5, 2008
Published online on December 17, 2007; doi: 10.1359/JBMR.071211

Role of *Bcl2* in Osteoclastogenesis and PTH Anabolic Actions in Bone

Junro Yamashita,[1,2] Nabanita S Datta,[2] Yong-Hee P Chun,[1] Dong-Ye Yang,[1] Allison A Carey,[2] Jaclynn M Kreider,[3] Steven A Goldstein,[3] and Laurie K McCauley[2,4]

ABSTRACT:

Introduction: B-cell leukemia/lymphoma 2 (*Bcl2*) is a proto-oncogene best known for its ability to suppress cell death. However, the role of *Bcl2* in the skeletal system is unknown. *Bcl2* has been hypothesized to play an important anti-apoptotic role in osteoblasts during anabolic actions of PTH. Although rational, this has not been validated in vivo; hence, the impact of *Bcl2* in bone remains unknown.
Materials and Methods: The bone phenotype of *Bcl2* homozygous mutant ($Bcl2^{-/-}$) mice was analyzed with histomorphometry and μCT. Calvarial osteoblasts were isolated and evaluated for their cellular activity. Osteoclastogenesis was induced from bone marrow cells using RANKL and macrophage-colony stimulating factor (M-CSF), and their differentiation was analyzed. PTH(1-34) (50 μg/kg) or vehicle was administered daily to $Bcl2^{+/+}$ and $Bcl2^{-/-}$ mice (4 days old) for 9 days to clarify the influence of *Bcl2* ablation on PTH anabolic actions. Western blotting and real-time PCR were performed to detect Bcl2 expression in calvarial osteoblasts in response to PTH ex vivo.
Results: There were reduced numbers of osteoclasts in $Bcl2^{-/-}$ mice, with a resultant increase in bone mass. $Bcl2^{-/-}$ bone marrow–derived osteoclasts ex vivo were significantly larger in size and short-lived compared with wildtype, suggesting a pro-apoptotic nature of $Bcl2^{-/-}$ osteoclasts. In contrast, osteoblasts were entirely normal in their proliferation, differentiation, and mineralization. Intermittent administration of PTH increased bone mass similarly in $Bcl2^{+/+}$ and $Bcl2^{-/-}$ mice. Finally, Western blotting and real-time PCR showed that Bcl2 levels were not induced in response to PTH in calvarial osteoblasts.
Conclusions: *Bcl2* is critical in osteoclasts but not osteoblasts. Osteoclast suppression is at least in part responsible for increased bone mass of $Bcl2^{-/-}$ mice, and *Bcl2* is dispensable in PTH anabolic actions during bone growth.
J Bone Miner Res 2008;23:621–632. Published online on December 17, 2007; doi: 10.1359/JBMR.071211

Key words: PTH, B-cell leukemia/lymphoma 2, anabolic, osteoclasts, osteoblasts

INTRODUCTION

The proto-oncogene, B-cell leukemia/lymphoma 2 (*Bcl2*), was originally identified in patients with follicular B-cell lymphoma where *Bcl2* is translocated to juxtapose with the immunoglobulin heavy chain locus, resulting in constitutive accumulation of their messenger RNA.[1] The oncogenic nature of *Bcl2* was shown in transgenic mice with lymphocyte targeted *Bcl2* gain of function where an extended B-cell lifespan and malignant lymphoma were noted.[2] Accumulating evidence indicates that *Bcl2* suppresses apoptosis in certain cells of the myeloid, lymphoid, and neuronal lineages.[3,4] A gene targeted mouse model in which *Bcl2* was inactivated showed a significant role of *Bcl2* in development of the lymphoid system.[5] *Bcl2* deficient ($Bcl2^{-/-}$) mice are viable at birth with a normal hematopoietic component initially, but are much smaller than their littermates, and with time, the number of lymphocytes is markedly decreased from peripheral blood because of apoptosis.[5] The exact mechanism for $Bcl2^{-/-}$ dwarfism is unknown. It could be attributed to the delay of growth plate turnover because *Bcl2* plays a role in growth plate chondrocytes.[6] However, considering that $Bcl2^{-/-}$ mice do not have a short-limb skeletal phenotype, but extreme smallness with normal body proportions, it is unlikely that the dwarfism is solely caused by a chondrodysplasia. Hence, *Bcl2* ablation likely has an impact on skeletal growth through its action in osteoclasts and/or osteoblasts.

Regulation of bone cell apoptosis holds tremendous therapeutic value for the treatment of osteoporosis.[7] In osteoporosis, osteoclast activity typically predominates

Dr McCauley receives unrelated clinical research grant support from Eli Lilly and has stock in Amgen. All other authors state that they have no conflicts of interest.

[1]Department of Biologic and Materials Sciences, University of Michigan School of Dentistry, Ann Arbor, Michigan, USA; [2]Department of Periodontics and Oral Medicine, University of Michigan, School of Dentistry, Ann Arbor, Michigan, USA; [3]Department of Orthopaedic Surgery, University of Michigan Medical School, Ann Arbor, Michigan, USA; [4]Department of Pathology, University of Michigan Medical School, Ann Arbor, Michigan, USA.

over osteoblast activity, resulting in a net decrease in bone mass. Therefore, suppression of osteoclast activity by promoting osteoclast apoptosis might be one strategy to increase bone mass. Similarly, enhancement of osteoblast activity by extending the lifespan of osteoblasts could result in a net increase in bone mass. Because *Bcl2* is associated with apoptosis, deregulated osteoclast and osteoblast apoptosis may contribute to development of the $Bcl2^{-/-}$ dwarfism. Osteoclasts are multinucleated cells derived from the myeloid lineage.[8] Recent findings suggest that early stage B lymphopoiesis may have a regulatory effect in osteoclastogenesis.[9,10] Furthermore, the subset of bone marrow B cells has been reported to hold potential to differentiate into osteoclasts in vitro.[11,12] Growing evidence indicates that osteoblasts play a pivotal role in the maintenance of hematopoietic stem cell (HSC) niche and myeloid differentiation.[13,14] Evidence shows that osteoblasts are necessary for the maturation of bone marrow B lymphopoiesis.[15] Therefore, a close relationship may exist between the B-lymphoid lineage and osteoclastogenesis. Because $Bcl2^{-/-}$ mice have defects in lymphopoiesis, one may speculate that osteoclast activity may also be deregulated. *Bcl2* has been reported to be an important regulator of apoptosis in osteoblasts as well.[16,17] Notably, *Bcl2* has been hypothesized to be a key molecule that mediates PTH-induced anti-apoptotic effects in osteoblasts.[18] PTH increases bone mass when administered intermittently,[19] and because of these anabolic actions, is now used for the treatment of postmenopausal osteoporosis in the United States.[20] However, the molecular mechanisms underlying the anabolic actions of PTH administration are unclear. One proposed mechanism is that PTH extends the lifespan of osteoblasts by upregulating *Bcl2* in a Runx2-dependent manner.[18,21] Activation of *Bcl2* would turn mature osteoblasts into long-living osteoblasts, resulting in enhanced bone formation. Although such a hypothesis is supported by in vitro studies,[18,22] it has not been confirmed through in vivo experiments. Hence, the role of *Bcl2* as a pivotal gene in apoptosis of osteoblasts during the anabolic actions of PTH in bone has not been validated.

In this study, the impact of *Bcl2* ablation was assessed on skeletal development to clarify the role of *Bcl2* in osteoclasts and osteoblasts. We further tested the hypothesis that *Bcl2* plays a critical function in the anabolic actions of PTH during bone growth. The study found that *Bcl2* plays a pivotal role in osteoclasts but not osteoblasts and that *Bcl2* is dispensable for the anabolic actions of PTH during bone growth.

MATERIALS AND METHODS

Phenotypic characterization of $Bcl2^{-/-}$ mice and TUNEL staining

Experimental protocols were approved, and all animals were treated in accordance with the guidelines of the University Committee on Use and Care of Animals of the University of Michigan. Mice heterozygous mutant for *Bcl2* (B6;129S2-*$Bcl2^{tm1Sjk}$*) were obtained from The Jackson Laboratory (Bar Harbor, ME, USA). Tail DNA genotyping was performed by PCR in the presence of *Bcl2* (5′-CTTTGTGGAACTGTACGGCCCCAGCATGCG-3′; 5′-ACAGCCTGCAGCTTTGTTTCATGGTACATC-3′) and *neo* sequences (5′-TCTGGACGAAGAGCATCAGGG-3′; 5′-CAAGCAGGCATCGCCATG-3′). Genotypes were confirmed by Western blotting of tissue lysate from the kidney. Microradiography of mice at day 11 was performed to evaluate the gross skeletal pattern. Body weight of mice was recorded daily from day 4 to day 13 after birth. For histological evaluation, paraffin sections were generated from the kidney and stained with H&E. Spleen from 13-day-old mice was paraffin-embedded and used to detect apoptosis using the In situ Cell Death Detection Assay (Roche, Penberg, Germany) following the manufacturer's instructions. Briefly, the sections were incubated with proteinase K. After rinsing with PBS, TUNEL reaction mixture was applied. The sections were counterstained with hematoxylin.

Flow cytometry

The bone marrow from the long bones of the day 13 mice was flushed with saline. Splenocytes were mechanically isolated by gently scraping spleen and passing cells through a needle. Mononuclear cells (1×10^6) were incubated with a combination of FITC-conjugated anti-mouse CD3 antibody and R-phycoerythrin (R-PE)–conjugated anti-mouse CD19 antibody, FITC-conjugated IgG and R-PE–conjugated IgG were used for isotype controls. Cell counting of $CD3^+$ and $CD19^+$ cells was performed using the BD FACSVantage system (BD Biosciences, Mountain View, CA, USA). All antibodies used in flow cytometry were purchased from BD Biosciences.

Tibias of $Bcl2^{-/-}$ mice, osteoclast perimeter, and TRACP5b

Formalin-fixed tibias of day 13 mice were decalcified in 10% EDTA, embedded in paraffin, and processed for H&E and TRACP staining. The Leukocyte Acid Phosphatase assay system (Sigma, St Louis, MO, USA) was used for TRACP staining. Digital photomicrographs of stained sections were histomorphometrically analyzed using Image-Pro Plus v4 (Media Cybernetics, Silver Spring, MD, USA). Because $Bcl2^{-/-}$ mice were smaller than $Bcl2^{+/+}$, a standardized area of interest was used for measuring bone area of tibias. The distance between the proximal and distal growth plates was first measured to calculate the proximal one third of the bone organ between the growth plates. This proximal one-third region was assessed for bone area (%). Osteoclast number and trabecular bone perimeter were calculated in the proximal tibia to determine osteoclast perimeters (#/mm). TRACP5b (a marker enzyme of bone resorption) was measured in the serum of day 13 mice using the MouseTRACP Assay (IDS, Boldon, UK).

Osteoclastogenesis and Bcl2 inhibitor ex vivo

The bone marrow of day 13 mice was flushed, and mononuclear cells were prepared by Ficoll gradient centrifugation. Cells were plated at 3×10^5 cells/cm^2 in 24-well plates in α-MEM (Invitrogen, Grand Island, NY, USA) supple-

mented with 10% FBS containing penicillin/streptomycin. Osteoclastogenesis was induced with 50 ng/ml RANKL (R&D Systems, Minneapolis, MN, USA) and 50 ng/ml macrophage-colony stimulating factor (M-CSF; R&D Systems). Medium was changed every 2 days. At days 5 and 9, cells were stained for TRACP activity. Number and total area (%) of $TRACP^+$ multinucleated cells (three or more nuclei per cell) were analyzed.

Flushed bone marrow from adult C57BL6 mice was cultured in Iscove's modified Dulbecco's medium (Invitrogen) supplemented with 20% FBS and 5 ng/ml of Flt3 ligand (R&D Systems) for 7 days as described.[23] The amplified hematopoietic cells were collected and plated at 1.8×10^5 cells/cm^2 in 24-well plates in α-MEM. Osteoclastogenesis was induced with RANKL and M-CSF. Medium was changed every 2 days. At day 4, cells were treated with a Bcl2 inhibitor (30 μM HA14-1; Tocris Biosciences, Ellisville, MO, USA) or vehicle (DMSO), and TRACP staining was performed at day 5 to enumerate osteoclasts.

Calvarial osteoblasts ex vivo

Calvariae of neonatal mice were dissected and subjected to four sequential 30-min digestions in collagenase A (2 mg/ml; Roche) with 0.25% trypsin. Cell fractions 2–4 were collected and plated in α-MEM. For enumeration, calvarial osteoblasts were plated at 1×10^4 cells/cm^2 in 24-well plates. Cell number was determined at days 1, 4, 7, and 10 by trypan blue exclusion and hemocytometer enumeration.

Calvarial osteoblasts were plated at 5×10^4 cells/cm^2 in 6-well plates in α-MEM. Medium was replaced with mineralization medium (α-MEM, 50 μg/ml ascorbic acid, 10 mM β-glycerophosphate) and cultured for 28 days. At day 29, cell layers were extracted with 15% trichloroacetic acid overnight. Insoluble material was removed by low-speed centrifugation. Supernatants were assayed for calcium with a commercially available kit (Pointe Scientific, Canton, MI, USA). DNA in pellets was extracted with the high salt method and quantified. Calcium was normalized to cellular DNA and expressed as units per microgram DNA. Alternatively, cell layers were stained for mineral using the von Kossa method. Briefly, cells were fixed in ethanol followed by incubation with 5% silver nitrate solution in the dark and exposed to a bright light.

Western blotting

The protein lysates from the kidneys were used to detect Bcl2 levels. SDS-PAGE was performed using 16% polyacrylamide gels to separate proteins and transferred to nitrocellulose membranes. The blots were blocked and incubated with mouse anti-Bcl2 (Santa Cruz Biotechnology, Santa Cruz, CA, USA) overnight at 4°C, and washed, followed by 1:10,000 horseradish peroxidase–conjugated anti-mouse IgG (Amersham Biosciences, Piscataway, NJ, USA). The protein bands were visualized by autoradiography using an enhanced chemiluminescence reagent (Pierce, Rockford, IL, USA). The blot was stripped and reprobed with mouse anti-α-tubulin (Sigma).

Calvarial osteoblasts were plated at 1×10^4 cells/cm^2 in α-MEM. At 70% confluency, cells were synchronized by serum starvation and cultured in α-MEM for 24 h. Collected cells were lysed in RIPA buffer, and protein concentration was determined. SDS-PAGE was performed, and proteins were blotted to nitrocellulose membranes. Mouse anti-cyclin D1 (Santa Cruz Biotechnology) was used for a primary antibody. After autoradiography, the blot was stripped and reprobed with anti-actin (Santa Cruz Biotechnology). Autoradiographs were digitized, and densitometry was performed to quantitatively measure the intensity of the bands using Image-Pro Plus.

Calvarial osteoblasts were treated with PTH(1-34) (10^{-7} M; Bachem, Torrence, CA, USA) to examine the impact of PTH on *Bcl2*. Ascorbic acid (50 μg/ml) was added to the culture medium 24 h before PTH treatment. Cells were treated with PTH for 0, 1, 2, 6, and 24 h. Western blotting to detect Bcl2 levels and densitometry was performed using mouse anti-Bcl2 and anti-α-tubulin (Sigma) antibodies.

Quantitative real-time PCR

Total RNA was extracted from cells using the RNeasy mini kit (Qiagen, Valencia, CA, USA). First-strand cDNA was synthesized using the SuperScript First-strand system (Invitrogen). Quantitative real-time PCR was performed using an iCycler IQ (BioRad, Hercules, CA, USA) with SYBRGreen mix (Invitrogen). Samples were run in triplicate, and results were normalized to GAPDH expression. The sets of primers used for real-time PCR were as follows: Bcl2, 5′-GGAAGGTAGTGTGTGTGG-3′ and 5′-ACTCCACTCTCTGGGTTCTTGG-3′; Runx2, 5′-CTGTGGTAACCGTCATGGCC and 5′-GGAGCTCGGCGGAGTAGTTC-3′; JunB, 5′-ATCAGCTACCTCCCACATGCA-3′ and 5′-TACGGTCTGCGGTTCCTCTT-3′.

Apoptosis assays

Thymocytes were mechanically isolated from the thymus of day 13 mice by gently scraping thymi in α-MEM and passing cells through a needle. Thymocytes were plated at 1×10^6 cells/ml in α-MEM and treated with dexamethasone (1 μM; Sigma) for 2 h. Calvarial osteoblasts were plated at 4×10^4 cells/cm^2 in α-MEM. Cells were treated with either dexamethasone (1 μM) for 3 days or staurosporine (0.1 μM; Sigma) for 24 h. Apoptosis was estimated by relative cell number using trypan blue exclusion. Alternatively, DNA fragmentation was analyzed using the TACS DNA laddering assay (R&D Systems) following the manufacturer's instructions. Five micrograms of genomic DNA was separated on a 1.2% agarose gel and laddering visualized by ethidium bromide staining.

Intermittent PTH administration and vossicle model

Bcl2$^{+/+}$ and *Bcl2*$^{-/-}$ mice (4 days old) received daily administration of either hPTH(1-34) (50 μg/kg) or vehicle (saline) for 9 days.[24] Because *Bcl2*$^{-/-}$ mice typically die at ~14 days of age, a 9-day PTH treatment was used in this study. Mice were killed at day 13.

The vertebrae of *Bcl2*$^{-/-}$ mice were implanted into immunocompromised mice, and PTH was administered daily to evaluate the effect of PTH on implant growth as de-

scribed before.[25] *Bcl2*$^{+/+}$ and *Bcl2*$^{-/-}$ (7 days old) mice were used as vertebrae donors, and immunocompromised mice (*Foxn1*^{nu}; Harlan, Indianapolis, IN, USA) were used as recipients. The lumbar vertebrae were removed and sectioned into single vertebral bodies (vossicles). Recipients were anesthetized with intraperitoneal injections of ketamine (90 mg/kg) and xylazine (5 mg/kg). The vossicles were subcutaneously implanted in the dorsal surface of recipients. Daily subcutaneous injection of either hPTH(1-34) (80 μg/kg) or vehicle was initiated a day after the surgery for 21 days. At day 22, vossicles were removed.

Histomorphometry and μCT

The tibias were removed and fixed in 10% formalin. The tibias were processed, paraffin embedded, sectioned, and stained for H&E and TRACP. Bone area (%) in the proximal one third of the bone organ between the growth plates, osteoblast perimeter (#/mm), and osteoclast perimeter (#/mm) in the metaphyseal compartment of the proximal tibias were assessed using Image-Pro Plus. μCT scanning was performed using an eXplore Locus SP cone beam MicroCT system (GE Healthcare Biosciences, London, Ontario, Canada). Image reconstruction was performed on 18-μm voxels, and a threshold was generated to select a mineralized tissue region using the MicroView Analysis+ (GE healthcare Biosciences). Bone volume fraction in the proximal one third of the bone organ between the growth plates was assessed.

Vossicles were decalcified, paraffin embedded, and processed with H&E staining for histomorphometry to measure total bone area (%). Alternatively, μCT scanning was carried out, and images were reconstructed in the same manner as described for the tibias. The trabecular region of the vossicles was delineated from the cortical shell and cartilage to assess the effect of PTH on trabecular bone.

Statistics

All data were analyzed for equality of variances. For parametric data, independent *t*-tests for two groups and ANOVA for multiple groups were performed. Tukey's test was used as a posthoc test. For nonparametric data, Kruskal-Wallis test was used. All statistical analysis was conducted with SPSS v12 (SPSS, Chicago, IL, USA). An α level of 0.05 was used. Results are presented as mean ± SE unless specified.

RESULTS

Validation and characterization of Bcl2$^{-/-}$ *mice*

Targeted deletion of the *Bcl2* gene was validated by PCR of tail DNA (Fig. 1A). Negative expression of Bcl2 protein was confirmed in *Bcl2*$^{-/-}$ kidney (Fig. 1B). *Bcl2*$^{-/-}$ mice typically fail to survive >2 wk after birth. The body size of *Bcl2*$^{-/-}$ mice at birth was similar to *Bcl2*$^{+/+}$; however, at day 11, it was evident that *Bcl2*$^{-/-}$ mice were significantly smaller than *Bcl2*$^{+/+}$ (Fig. 1C). Body weight was measured from day 4 to day 13, and average weight was plotted. *Bcl2*$^{-/-}$ mice gained little weight after day 7, whereas *Bcl2*$^{+/+}$ mice gained weight consistently during the observation period (Fig. 1D). Kidney and spleen were harvested from 13-day-old mice for histological evaluation. H&E staining of *Bcl2*$^{-/-}$ kidneys showed severe generalized cystic lesions in the entire kidney compared with *Bcl2*$^{+/+}$ (Fig. 1E). TUNEL staining of spleen sections was performed to detect apoptotic cells. A large number of TUNEL^{+} cells were detected in *Bcl2*$^{-/-}$ spleen sections, whereas very few TUNEL^{+} cells were found in *Bcl2*$^{+/+}$ spleen sections (Fig. 1F).

Hematopoietic component of Bcl2$^{-/-}$ *bone marrow was altered*

To characterize lymphocytes in the bone marrow and spleen, flow cytometric analysis was performed. Results are summarized in Figs. 2A and 2B. The ratio of B cells to total mononuclear cells in *Bcl2*$^{-/-}$ bone marrow was significantly reduced compared with *Bcl2*$^{+/+}$. There was a tendency of reduced numbers of B cells in *Bcl2*$^{-/-}$ versus *Bcl2*$^{+/+}$ spleens, but this was not statistically significant. A similar pattern was observed for T lymphocytes. The T-cell ratio to total mononuclear cells in *Bcl2*$^{-/-}$ was considerably smaller than that in *Bcl2*$^{+/+}$, whereas no statistical difference was found between *Bcl2*$^{+/+}$ and *Bcl2*$^{-/-}$ in T cells in the spleen. Thus, lymphopoiesis in the bone marrow but not in the spleen was impaired in *Bcl2*$^{-/-}$ mice.

Increased bone mass and decreased osteoclast number in Bcl2$^{-/-}$ *tibias*

Representative photomicrographs of tibias from day 13 mice are shown in Fig. 2C. Histomorphometric analysis of the metaphyseal compartment showed that *Bcl2*$^{-/-}$ tibias had significantly greater percent bone areas (25.5 ± 0.7%; amount of bone tissue per total bone organ) compared with *Bcl2*$^{+/+}$ (20.5 ± 1.6%). No difference was noted in osteoblast perimeter in the metaphyseal compartment of the proximal tibias between *Bcl2*$^{+/+}$ (17.2 ± 2.0 #/mm) and *Bcl2*$^{-/-}$ (15.5 ± 1.6 #/mm). TRACP staining showed considerably lower osteoclast number in *Bcl2*$^{-/-}$ tibias versus *Bcl2*$^{+/+}$ (Fig. 2D). Consistent with this, serum TRACP5b levels were significantly lower in *Bcl2*$^{-/-}$ compared with *Bcl2*$^{+/+}$ (Fig. 2E). These results indicate that osteoclast activity was compromised in *Bcl2*$^{-/-}$ bone.

Altered osteoclastogenesis in Bcl2$^{-/-}$ *bone marrow ex vivo*

Because *Bcl2*$^{-/-}$ mice exhibited significantly fewer osteoclasts, the role of *Bcl2* in osteoclastogenesis and osteoclast survival was studied. Osteoclastogenesis was induced in bone marrow mononuclear cell cultures using RANKL and M-CSF. A significant difference was found between *Bcl2*$^{+/+}$ and *Bcl2*$^{-/-}$ during a course of osteoclastogenesis. Enumeration of osteoclasts showed that, at day 5, significantly more osteoclasts were present in *Bcl2*$^{-/-}$ cell cultures (Fig. 3A). However, the number of osteoclasts significantly dropped during the period of day 5 to day 9 in *Bcl2*$^{-/-}$ versus *Bcl2*$^{+/+}$ cultures (Fig. 3B). Another prominent difference was osteoclast size. *Bcl2*$^{-/-}$ osteoclasts were much larger than *Bcl2*$^{+/+}$ osteoclasts at day 5 (Figs. 3C and 3D). The size of *Bcl2*$^{-/-}$ osteoclasts was approximately two times larger than that of *Bcl2*$^{+/+}$. At day 9, the size was similar

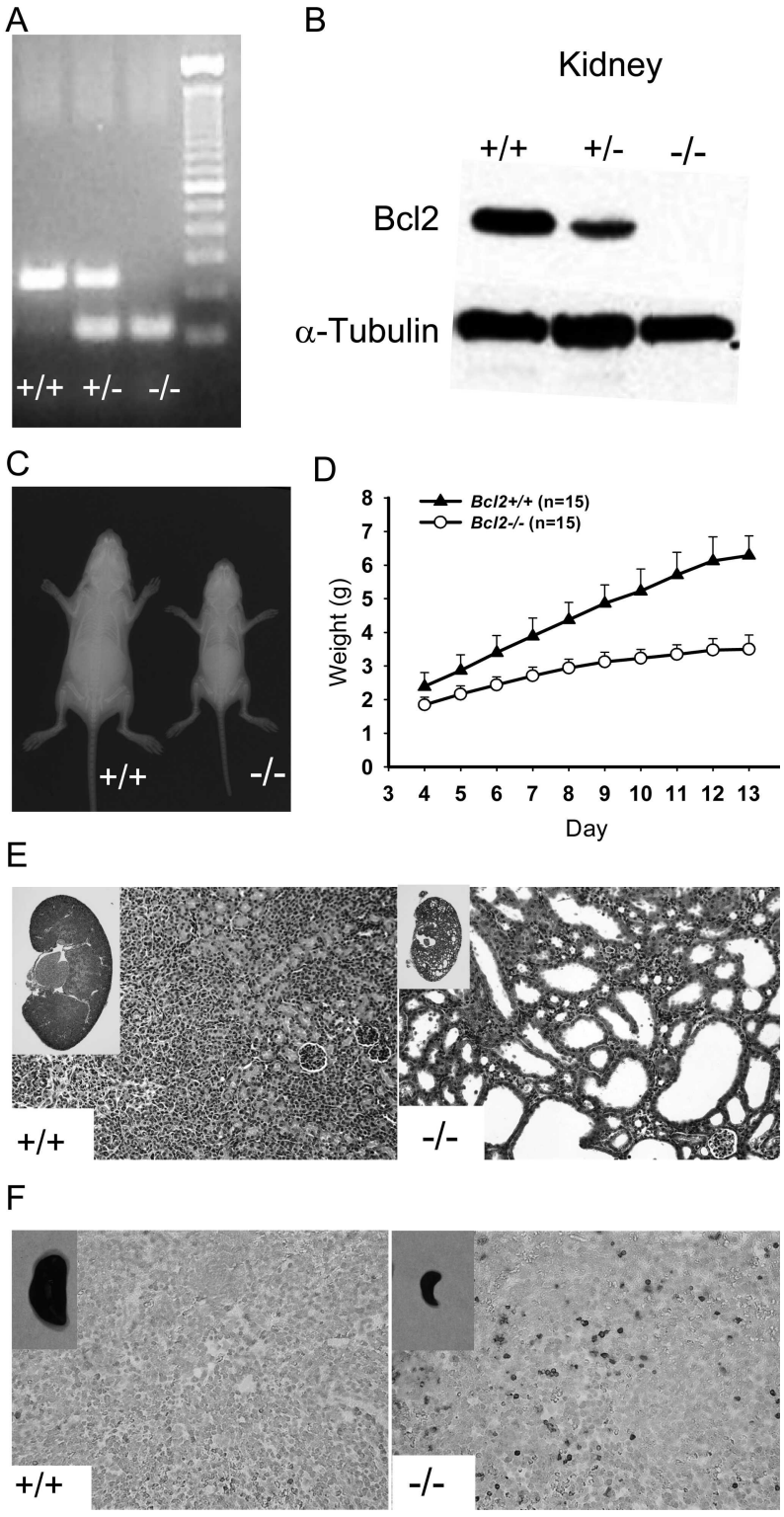

FIG. 1. Characterization of *Bcl2*$^{-/-}$ mice. (A) Tail DNA genotyping. (B) The absence of Bcl2 protein was confirmed by Western analysis. (C) At day 11, *Bcl2*$^{-/-}$ mice were significantly smaller than their littermates. (D) Weight change over 9 days starting at day 4. *Bcl2*$^{-/-}$ mice gained on average as little as 1 g in weight, whereas *Bcl2*$^{+/+}$ gained >3.5 g. Results are presented as mean ± SD. (E) H&E staining of the kidney sections, ×200. *Bcl2*$^{-/-}$ mice develop severe polycystic kidneys. (F) TUNEL staining of the spleen sections, ×200. Dark brown–stained cells indicate apoptosis. Numerous apoptotic splenocytes were observed in *Bcl2*$^{-/-}$ spleen.

between *Bcl2*$^{+/+}$ and *Bcl2*$^{-/-}$, because the *Bcl2*$^{-/-}$ osteoclasts were much smaller than at day 5.

Bcl2 inhibitor impaired osteoclastogenesis ex vivo

Wildtype osteoclasts and pre-osteoclasts were treated with the Bcl2 inhibitor (antisense oligonucleotide, HA14-1) to further explore the role of *Bcl2* in osteoclasts. The Flt3 ligand-expanded hematopoietic cells from C57BL6 mice were cultured with RANKL and M-CSF for 5 days. Cells were treated with HA14-1 24 h before TRACP staining. HA14-1 significantly suppressed osteoclast number compared with vehicle-treated cells (Fig. 3E).

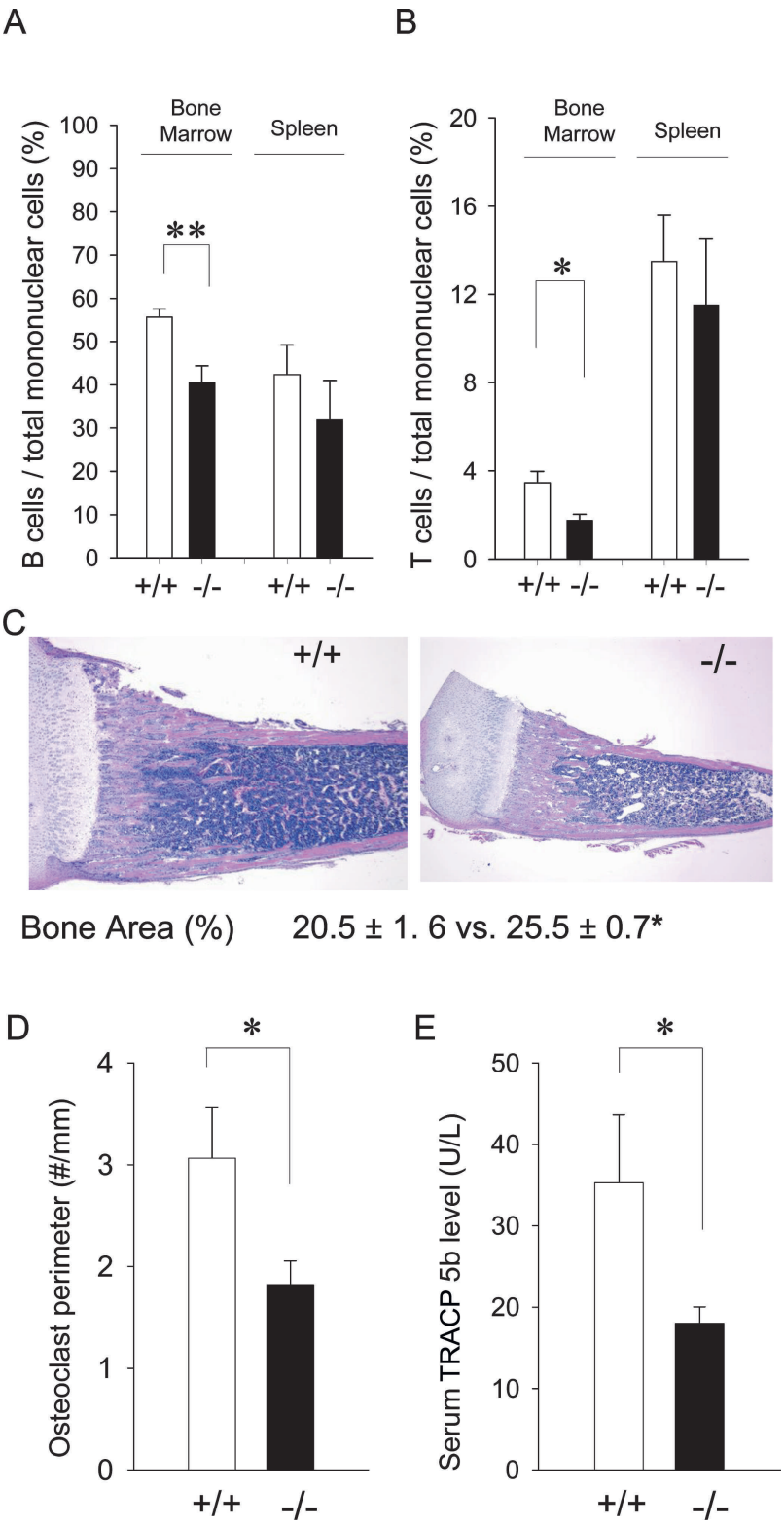

FIG. 2. Altered hematopoietic component, decreased osteoclast density, and increased bone mass in $Bcl2^{-/-}$ bone. Mononuclear cells from the bone marrow and spleen were stained with CD3 and CD19 antibodies. Flow cytometry was performed to detect $CD3^+$ and $CD19^+$ cells ($n > 6$ /group). (A) The B-cell ratio was significantly reduced in $Bcl2^{-/-}$ vs. $Bcl2^{+/+}$ bone marrow, whereas in the spleen, no significant difference was observed. (B) The T-cell ratio was significantly reduced in $Bcl2^{-/-}$ bone marrow compared with that of $Bcl2^{+/+}$ but not in the spleen. (C) The proximal one third of the bone organ between the growth plates was histomorphometrically analyzed. Significantly higher bone areas (%) were found in $Bcl2^{-/-}$ tibias than $Bcl2^{+/+}$ ($n = 5$/group). (D) Osteoclast numbers per linear perimeter were significantly less in $Bcl2^{-/-}$ than $Bcl2^{+/+}$ ($n > 8$/group). (E) Similarly, serum TRACP5b levels in $Bcl2^{-/-}$ mice were considerably lower than that in $Bcl2^{+/+}$ ($n > 7$/group). $*p < 0.05$, $**p < 0.01$ ($Bcl2^{-/-}$ vs. $Bcl2^{+/+}$).

Role of Bcl2 in osteoblasts ex vivo

To elucidate how *Bcl2* deletion affects the cellular activities of osteoblasts ex vivo, enumeration, proliferation, and mineralization assays were carried out with calvarial osteoblasts. Enumeration of $Bcl2^{-/-}$ osteoblasts over time were comparable to that of $Bcl2^{+/+}$ (Fig. 4A). Western blot analysis for the cell cycle gene, cyclin D1, showed that cyclin D1 was similar in $Bcl2^{-/-}$ to that in $Bcl2^{+/+}$ (Fig. 4B). Densitometric analysis showed no statistical difference in cyclin D1

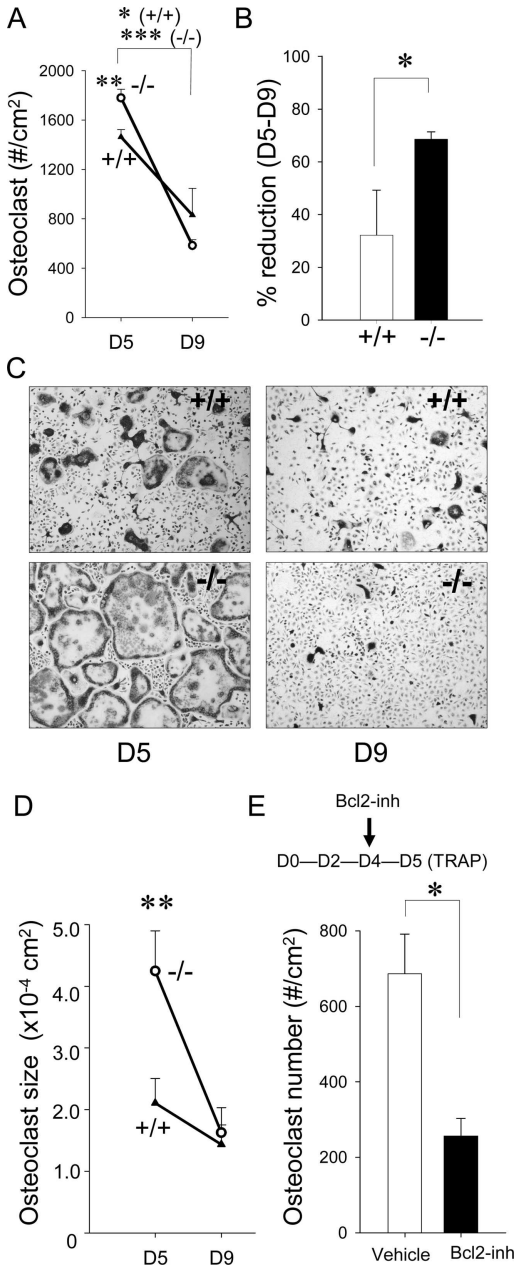

FIG. 3. *Bcl2*$^{-/-}$ osteoclasts were large and short lived ex vivo. Osteoclastogenesis was induced from bone marrow mononuclear cells with RANKL and M-CSF. (A) At day 5, osteoclast numbers per square centimeter were significantly higher in *Bcl2*$^{-/-}$ than *Bcl2*$^{+/+}$. At day 9, no difference was detected between *Bcl2*$^{+/+}$ and *Bcl2*$^{-/-}$ ($n > 5$/group). (B) *Bcl2*$^{-/-}$ osteoclast number dropped from day 5 to day 9 more significantly than *Bcl2*$^{+/+}$ osteoclast number ($n > 5$/group). (C) Representative micrographs of TRACP-stained bone marrow cell cultures. The size of *Bcl2*$^{-/-}$ osteoclasts was larger than *Bcl2*$^{+/+}$ at day 5. At day 9, *Bcl2*$^{-/-}$ osteoclasts were much smaller than at day 5. No difference was noted in osteoclast size between genotypes at day 9. (D) Surface area of osteoclasts per well was determined and normalized by cell numbers per well. At day 5, *Bcl2*$^{-/-}$ osteoclasts were significantly larger than *Bcl2*$^{+/+}$ osteoclasts. However, at day 9, osteoclasts from both genotypes were small, and no difference was found between genotypes ($n > 5$/group). (E) The Bcl2 inhibitor HA14-1 significantly suppressed osteoclastogenesis in wildtype hematopoietic cell cultures ($n = 3$/group). *$p < 0.05$, **$p < 0.01$, ***$p < 0.001$.

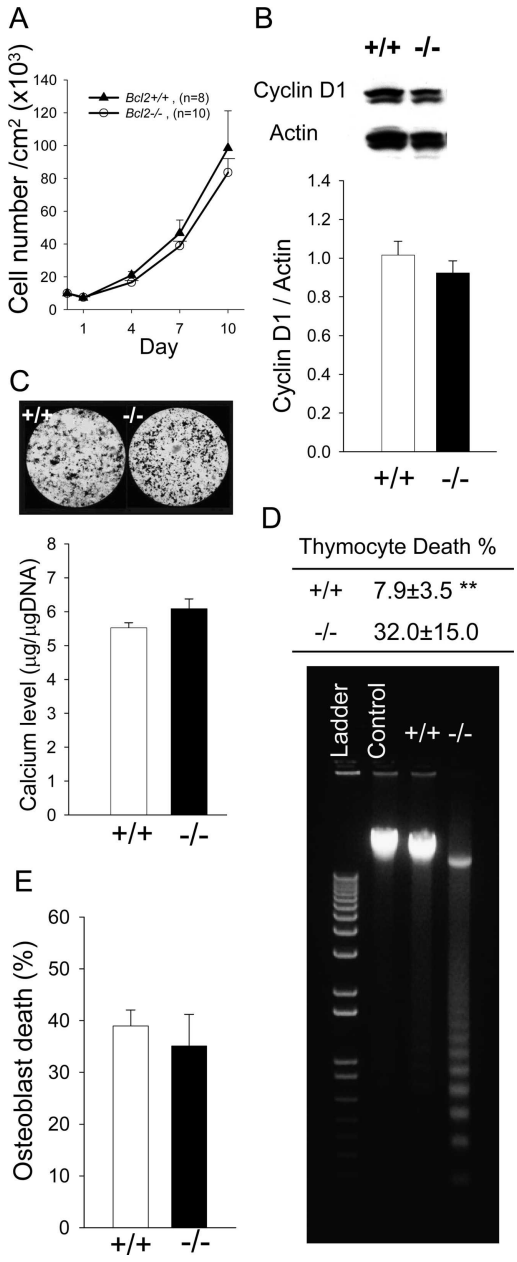

FIG. 4. Characterization of calvarial osteoblasts. (A) Calvarial osteoblasts were plated at 10,000 cells/cm^2, and cell numbers were determined every 3 days. No difference was detected in cell numbers over time between genotypes. (B) Cell growth was synchronized and protein was extracted after serum stimulation for analysis. No significant difference was found in cyclin D1 levels between *Bcl2*$^{+/+}$ and *Bcl2*$^{-/-}$ osteoblasts ($n > 7$/group). (C) Cells were cultured in mineralization medium for 28 days. Representative images of Von Kossa staining are shown. Calcium levels normalized by total DNA were statistically analyzed ($n > 10$/group). No difference was noted in calcium levels between *Bcl2*$^{+/+}$ and *Bcl2*$^{-/-}$ cultures. (D) Thymocytes were treated with dexamethasone for 2 h. Cell death was estimated by relative cell number vs. control. Significant cell death was noted in *Bcl2*$^{-/-}$ thymocytes ($n > 5$/group). Considerable DNA fragmentation occurred in *Bcl2*$^{-/-}$ thymocytes compared with *Bcl2*$^{+/+}$. (E) Calvarial osteoblasts were treated with staurosporine for 24 h. Cell number was determined with trypan blue exclusion. No difference was found in numbers of nonviable cells between *Bcl2*$^{+/+}$ and *Bcl2*$^{-/-}$ osteoblasts ($n > 5$/group). **$p < 0.01$.

expression between $Bcl2^{+/+}$ and $Bcl2^{-/-}$, suggesting that their proliferation activities were equivalent. $Bcl2^{-/-}$ osteoblasts formed mineralized nodules similar to $Bcl2^{+/+}$ osteoblasts (Fig. 4C). To quantify mineralization, calcium levels were normalized by total DNA. Statistical analysis showed that there was no difference in mineralization activity between $Bcl2^{+/+}$ and $Bcl2^{-/-}$ osteoblasts. These ex vivo assays indicated that the absence of *Bcl2* did not play a major role in normal osteoblast enumeration, proliferation, or mineralization.

Bcl2 is critical in thymocyte but not in osteoblast apoptosis

To assess the role of *Bcl2* in apoptosis, thymocytes and osteoblasts were stimulated with dexamethasone and staurosporine. Dexamethasone induced significantly greater apoptosis in $Bcl2^{-/-}$ thymocytes compared with $Bcl2^{+/+}$ (Fig. 4D). DNA laddering confirmed that dexamethasone induced considerable DNA fragmentation in $Bcl2^{-/-}$ thymocytes. Staurosporine for 24 h induced apoptosis in osteoblasts of both genotypes, but there was no significant difference in cell death rate between $Bcl2^{+/+}$ and $Bcl2^{-/-}$ (Fig. 4E).

Intermittent PTH administration increased bone mass in $Bcl2^{-/-}$ tibias

To elucidate the impact of *Bcl2* on PTH anabolic actions in intact mice, PTH was administered intermittently to $Bcl2^{+/+}$ and $Bcl2^{-/-}$ mice. Intermittent PTH administration increased bone mass of the proximal tibias significantly regardless of genotype (Fig. 5A). μCT scanning confirmed that $Bcl2^{-/-}$ mice responded to intermittent PTH in an anabolic mode (Fig. 5B). A significantly higher bone volume fraction was noted in the tibias of both PTH-administered $Bcl2^{+/+}$ and $Bcl2^{-/-}$ mice compared with respective vehicle controls. Consistently, osteoblast perimeter (#/mm) was significantly higher in both PTH administered $Bcl2^{+/+}$ and $Bcl2^{-/-}$ mice (42.6 ± 1.5 and 40.4 ± 1.0, respectively) compared with respective controls (17.2 ± 2.0 and 15.5 ± 1.6). No difference was found between $Bcl2^{+/+}$ and $Bcl2^{-/-}$ with respect to PTH anabolic actions; both genotypes responded similarly to intermittent PTH. These in vivo experiments showed that daily PTH administration for 9 days dramatically increased bone mass in the tibias regardless of genotype.

Daily PTH administration enhanced bone formation in $Bcl2^{-/-}$ vossicles

Because $Bcl2^{-/-}$ mice develop kidney failure, endocrine dysfunction in $Bcl2^{-/-}$ mice could influence the outcome of in vivo PTH therapy. To rule out the possible effect of kidney failure, a vossicle implant experiment was performed.[25] Using this model, the interaction between hematopoietic (host origin) and mesenchymal cells (donor origin) can be assessed in addition to obviating the potential systemic impact of the kidney phenotype and subsequent lethality of *Bcl2* ablation.

H&E staining of vossicle sections showed enhanced trabecular bone in PTH-administered mice, regardless of genotype (Fig. 5C). PTH administration enhanced bone in vossicles with fine trabeculation regardless of genotype, whereas vossicles in the vehicle control group exhibited considerably less trabecular bone in both genotypes. The result of μCT scanning of vossicles confirmed that intermittent PTH administration increased bone mass in both $Bcl2^{+/+}$ and $Bcl2^{-/-}$ vossicles. Whereas the vossicles from PTH-administered mice had dense trabecular structure, vossicles from vehicle-treated mice had little trabecular structure (Fig. 5D). To study the effect of PTH on trabecular bone, cartilage, and cortical shells were excluded from μCT data for analysis. Trabecular bone volume fraction (%) of vossicles in PTH-administered mice was significantly higher than that of vehicle. The degree of such increase was similar between $Bcl2^{+/+}$ and $Bcl2^{-/-}$. Thus, intermittent PTH administration significantly increased net bone mass in both $Bcl2^{+/+}$ and $Bcl2^{-/-}$ vossicles.

PTH effect on Bcl2 in calvarial osteoblasts

It has been reported that PTH induces *Bcl2* in a Runx2-dependent manner in the osteoblastic cell line, OB-6.[18] To determine whether PTH induces *Bcl2* in primary osteoblasts, calvarial osteoblasts from $Bcl2^{+/+}$ mice were treated with PTH and analyzed for Bcl2 protein expression. As a positive control for the PTH response in osteoblasts, the immediate early gene, *JunB*, was also analyzed. The result of Western blotting showed that Bcl2 was not induced in calvarial osteoblasts (Fig. 6A). PTH-induced JunB expression followed a pattern typical to that previously published.[26] JunB expression was high a few hours after PTH stimulation and significantly decreased after 6 h. Such a typical expression pattern of JunB by PTH treatment confirms that calvarial osteoblasts responded to PTH. The result of protein analysis was further verified by assessing the relative expression of *Bcl2*, *Runx2*, and *JunB* at the RNA level using real-time PCR. There was no significant upregulation of *Bcl2* or *Runx2* in response to PTH in osteoblasts, whereas *JunB* was significantly induced after 1 h PTH treatment (Fig. 6B).

DISCUSSION

$Bcl2^{-/-}$ mice had increased bone mass and altered bone marrow hematopoietic components versus wildtype mice. The ratios of both B cells and T cells to total mononuclear cells were significantly reduced in $Bcl2^{-/-}$ mice and decreased osteoclast numbers were found in $Bcl2^{-/-}$ bone. Consistently, serum TRACP5b levels were significantly lower in $Bcl2^{-/-}$ mice. Thus, lymphopoiesis and osteoclastogenesis were both weakened in $Bcl2^{-/-}$ bone marrow. There was no alteration in proliferation or mineralization of $Bcl2^{-/-}$ osteoblasts, suggesting *Bcl2* is not critical for the osteoblast phenotype. Boot-Handford et al.[27] reported that $Bcl2^{-/-}$ mice had increased osteoblast numbers, and the shape of osteoblasts was more cuboidal than wildtype. In this study, no noticeable difference was observed in osteoblast numbers or morphology. This discrepancy in observation could reflect a difference in mouse strain or tech-

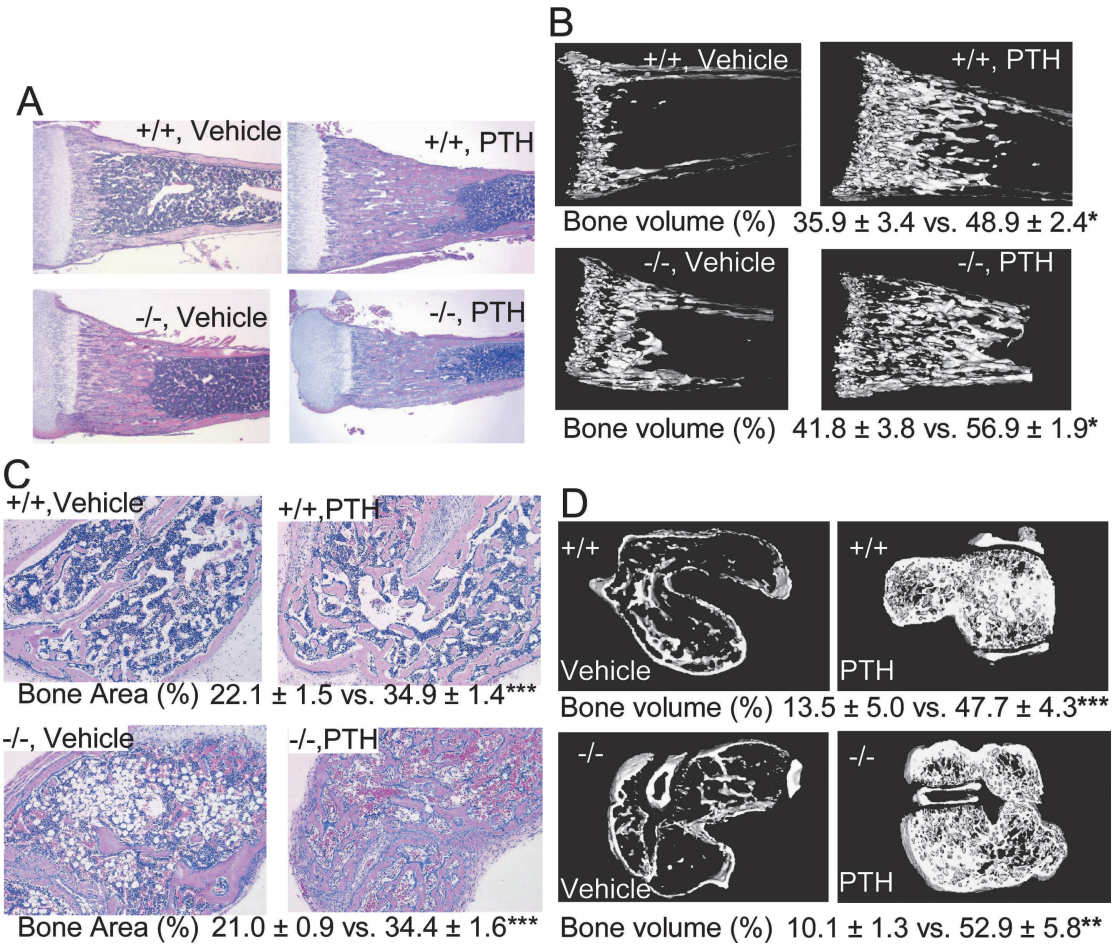

FIG. 5. Intermittent PTH increased bone mass in $Bcl2^{-/-}$ tibias and vossicles. PTH was administered daily to $Bcl2^{+/+}$ and $Bcl2^{-/-}$ mice from day 4 to day 12, and the proximal one third of each tibia was selected for analysis. (A) Representative micrographs of H&E-stained tibias. Substantial trabecular bone was noted in PTH-administered groups regardless of genotype ($n > 15$/group). (B) Representative μCT images with summary data below. In both genotypes, considerably more trabecular bone was found in PTH-administered groups vs. controls ($n = 5$/group). Regardless of genotype, intermittent PTH administration induced significantly higher bone volume fraction than vehicle. (C) Vertebrae from $Bcl2^{+/+}$ and $Bcl2^{-/-}$ mice were subcutaneously implanted into athymic mice, and PTH was administered daily for 21 days. Representative micrographs of H&E-stained vossicle sections with summary data below. Enhanced trabeculation was found in PTH-administered groups regardless of genotype. Controls exhibit sparse trabeculation in both genotypes. Bone area (%) was significantly higher in the PTH-administered group than vehicle control regardless of genotype. No difference was found in bone area (%) between $Bcl2^{+/+}$ and $Bcl2^{-/-}$, irrespective of treatment ($n > 23$/group). (D) Representative μCT images with summary statistics below. Intermittent PTH administration significantly enhanced bone in vossicles of both genotypes. Little trabecular structure was noted in controls regardless of genotype ($n = 4$/group). $^*p < 0.05$, $^{**}p < 0.01$, $^{***}p < 0.001$.

niques used. The quantitative measures used in this study were also more extensive than those used in the former study.

Significant differences were identified in osteoclastogenesis ex vivo. $Bcl2^{-/-}$ osteoclastogenesis was rapid and robust, but also vanished rapidly thereafter, whereas $Bcl2^{+/+}$ osteoclastogenesis developed more gently and remained active for a longer period than $Bcl2^{-/-}$. Moreover, when the burst of $Bcl2^{-/-}$ osteoclastogenesis took place, osteoclasts were much larger compared with $Bcl2^{+/+}$ counterparts. This distinctive feature of $Bcl2^{-/-}$ osteoclastogenesis suggests a critical role of *Bcl2* in regulation of osteoclast fusion and apoptosis. Osteoclasts typically have a short lifespan.[28] Apoptosis occurs rapidly after the removal of trophic factors such as M-CSF in vitro.[29] Although the significance of osteoclast fusion remains mostly unknown, osteoclast survival is considered to depend on continued replenishment by fusion.[28] It is known that *Bcl2* activation promotes survival of certain cells in the myeloid and lymphoid lineages.[3] Because osteoclasts are of hematopoietic origin and share some features with bone marrow macrophage/monocytes,[30] *Bcl2* activation may contribute to osteoclast survival as well. Indeed, our ex vivo finding that the *Bcl2* inhibitor significantly suppressed osteoclast survival supports a critical role of *Bcl2* in osteoclast survival. Therefore, the cell autonomous change in $Bcl2^{-/-}$ osteoclasts is likely responsible at least in part for the increased bone mass in $Bcl2^{-/-}$ mice. McGill et al.[31] reported that *microphthalmia* (*Mitf*) regulates *Bcl2* in melanocytes and osteoclasts and that the osteopetrotic phenotype of $Mitf^{mi/mi}$ mice is par-

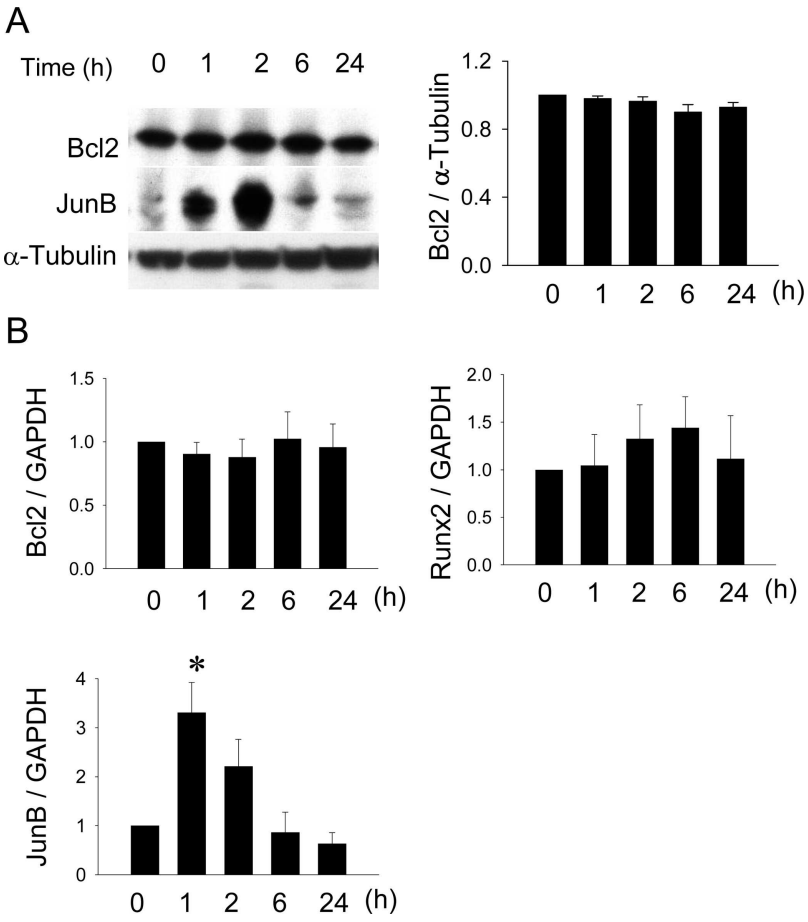

FIG. 6. Lack of PTH-mediated increase in Bcl2 ex vivo. Calvarial osteoblasts were treated with PTH (10^{-7} M) for the indicated time course. (A) Protein was extracted and analyzed for Bcl2. JunB expression was detected to verify PTH activity in osteoblasts. Densitometry was carried out and analyzed ($n = 5$ for each). No significant difference in PTH-induced Bcl2 expression was found during the time course, whereas PTH-induced JunB expression followed an expected pattern. (B) Total RNA was extracted and analyzed for *Bcl2*, *Runx2*, and *JunB* using quantitative real-time PCR. PTH did not induce *Bcl2* nor *Runx2*, but significantly higher *JunB* expression was noted with 1 h of PTH treatment.

tially attributed to deregulation of *Bcl2*. In that report, the osteopetrotic phenotype of *Bcl2*$^{-/-}$ mice was shown with no insight to explain the phenotypic change. Our result is accordant with their findings and provides analytical explanation. Impaired osteoclastogenesis could result from lymphopenia because lymphocytes are sources of RANKL.[9,11] Because lymphopoiesis of *Bcl2*$^{-/-}$ mice is normal at birth[5] and hence lymphopenia developed in a short period in this study (maximum 13 days), it is unlikely that acute lymphopenia solely caused the increased bone mass by suppressing osteoclastogenesis.

Bcl2 is a crucial gene in thymocyte apoptosis but may not play an important role in osteoblast apoptosis stimulated by dexamethasone or staurosporine. Dexamethasone induced significantly higher apoptosis in *Bcl2*$^{-/-}$ thymocytes compared with *Bcl2*$^{+/+}$, whereas no noticeable dexamethasone-induced apoptosis was observed in osteoblasts from either genotype during 3 days of incubation (data not shown). Glucocorticoids are widely used for the treatment of inflammatory and autoimmune diseases and lymphomas. They are known to suppress the host immune response and induce apoptosis in lymphocytes.[32] In bone, the long-term use of glucocorticoids often results in bone loss.[33] It has been shown that dexamethasone treatment induces apoptosis in osteoblasts in vivo[16,34] and in vitro.[35] Our result that *Bcl2*$^{-/-}$ thymocytes were susceptible to dexamethasone-induced apoptosis is consistent with a previous report,[5] but the observation in primary osteoblasts was not. This is likely because dexamethasone is a mild apoptosis inducer compared with other chemotherapeutic agents such as etoposide.[36] Therefore, staurosporine was used to induce osteoblast apoptosis. Staurosporine induced apoptosis in osteoblasts; however, no significant difference was noted between *Bcl2*$^{+/+}$ and *Bcl2*$^{-/-}$. This suggests that the absence of *Bcl2* does not affect apoptosis in osteoblasts. It is possible that the activation of apoptosis-related genes may be redundant in osteoblasts. Alternative genes may be upregulated to compensate for the functional loss of *Bcl2* to maintain the anti-apoptotic to apoptotic ratio in a cell. Further research is needed to elucidate the mechanism of osteoblast apoptosis.

Bcl2 has been proposed as a candidate that renders osteoblasts anti-apoptotic in a Runx2-dependent manner in response to PTH, thereby enhancing bone formation.[18] Intermittent PTH administration to *Bcl2*$^{-/-}$ mice in this study dramatically increased bone mass in their trabecular compartments, at a comparable level to that seen in wild-type littermates. Because this study did not focus specifically on apoptosis of osteoblasts but the overall role of *Bcl2* in PTH anabolic action, it is difficult to address whether apoptosis of osteoblasts plays a role in PTH actions. Nonetheless, an inference can be made from the in vivo part of this study that *Bcl2* is not likely the critical mediator of anti-apoptotic signaling in osteoblasts nor does PTH acti-

vate *Bcl2* to inhibit osteoblast apoptosis. Because PTH has been shown to have pro- and anti-apoptotic actions in osteoblasts,[21,37] the hypothesis that osteoblast apoptosis plays a role in PTH anabolic action[21] is rational, and it has been anticipated that the inhibition of osteoblast apoptosis would lead to a clinical strategy to increase the bone mass.[7] It is possible that different results could be obtained in a model of osteoporosis such as sex steroid withdrawal compared with the bone growth models used in this study. On the other hand, several lines of evidence have indicated that osteoblast apoptosis is an important component of mineralization in vitro and normal bone formation in vivo.[17,38] It was shown that intermittent PTH administration transiently increased numbers of apoptotic osteoblasts and osteocytes in rat trabecular bone, but no protection from apoptosis was observed during the course of PTH treatment.[39] This study found that PTH did not regulate the apoptosis-related gene *Bcl2*. Similar findings were shown in a microarray study that compared gene expression in bone between continuous and intermittent PTH administration.[40] This microarray study failed to detect upregulation of *Bcl2* and other apoptosis-related genes in the intermittent PTH group. Lindsay et al.[41] studied the effect of PTH treatment on bone of patients with osteoporosis and found that enhanced bone formation was associated with an increase in osteoblast apoptosis. Our finding that *Bcl2* is not essential in PTH action in vivo is consistent with these studies. Moreover, our in vivo finding is reinforced by our ex vivo result where PTH did not induce *Bcl2* or *Runx2* in calvarial osteoblasts.

This study used a global knockout mouse model of *Bcl2*. Polycystic kidney disease is a prominent feature in $Bcl2^{-/-}$ mice. Kidney failure induces renal osteodystrophy in which bone is generally osteopenic because of enhanced osteoclast activity.[42] In this study, $Bcl2^{-/-}$ mice showed higher bone mass with decreased osteoclast numbers. Sorensen et al.[43] reported that kidneys from newborn $Bcl2^{-/-}$ mice were not cystic but small, and as the mice grew, the kidneys became cystic. Therefore, the systemic effect of acute renal failure in our $Bcl2^{-/-}$ mice was not likely significant at day 13. Rather, cell autonomous changes in osteoclasts caused by *Bcl2* ablation likely played a major role in the bone phenotype of $Bcl2^{-/-}$ mice. Because the kidney is a crucial organ for calcium reabsorption that is partly under the hormonal control of PTH, $Bcl2^{-/-}$ mice may have fluctuating endogenous PTH levels that may affect the experimental outcome. However, in the vossicle implant system, the hematopoietic components come from the host (athymic mice). Hence, no effect of fluctuating endogenous PTH or compromised kidney function would be expected in the vossicle response in this study. Daily PTH administration increased bone mass in vossicles significantly regardless of genotype. The consideration that $Bcl2^{+/+}$ stromal progenitors could migrate into vossicles from the host through blood vessels is possible; however, we found in a similar model system that PTH was unable to mobilize host cells to implants.[44] Therefore, the result from the vossicle experiment reinforces our finding that *Bcl2* is dispensable in PTH anabolic actions. Interestingly, considering that the intact $Bcl2^{-/-}$ mice responded to PTH with increased bone, this study also validated that PTH anabolic actions are not dependent on the presence of a normally functioning kidney or physiologic increases in body weight/size. Despite that the mice failed to normally increase body weight during growth, they maintained a robust skeletal response to PTH.

This study showed that *Bcl2* is critical in maturation of osteoclasts but not in osteoblasts. Suppressed osteoclasts in $Bcl2^{-/-}$ bone marrow are at least in part responsible for the high bone mass of $Bcl2^{-/-}$ mice. Evidence was also found that *Bcl2* is dispensable in PTH anabolic action in bone.

ACKNOWLEDGMENTS

The authors thank Akihiro Yamashita for osteoclast analysis. This study was supported by the National Institutes of Health DK53904, CA093900, the University of Michigan musculoskeletal Core Center P30-AR46024, and OVPR #5534.

REFERENCES

1. Tsujimoto Y, Cossman J, Jaffe E, Croce CM 1985 Involvement of the bcl-2 gene in human follicular lymphoma. Science **228:**1440–1443.
2. McDonnell TJ, Korsmeyer SJ 1991 Progression from lymphoid hyperplasia to high-grade malignant lymphoma in mice transgenic for the t(14; 18). Nature **349:**254–256.
3. Vaux DL, Cory S, Adams JM 1988 Bcl-2 gene promotes haemopoietic cell survival and cooperates with c-myc to immortalize pre-B cells. Nature **335:**440–442.
4. Garcia I, Martinou I, Tsujimoto Y, Martinou JC 1992 Prevention of programmed cell death of sympathetic neurons by the bcl-2 proto-oncogene. Science **258:**302–304.
5. Veis DJ, Sorenson CM, Shutter JR, Korsmeyer SJ 1993 Bcl-2-deficient mice demonstrate fulminant lymphoid apoptosis, polycystic kidneys, and hypopigmented hair. Cell **75:**229–240.
6. Amling M, Neff L, Tanaka S, Inoue D, Kuida K, Weir E, Philbrick WM, Broadus AE, Baron R 1997 Bcl-2 lies downstream of parathyroid hormone-related peptide in a signaling pathway that regulates chondrocyte maturation during skeletal development. J Cell Biol **136:**205–213.
7. Manolagas SC 2000 Birth and death of bone cells: Basic regulatory mechanisms and implications for the pathogenesis and treatment of osteoporosis. Endocr Rev **21:**115–137.
8. Takahashi N, Udagawa N, Takami M, Suda T 2002 Cells of bone, osteoclast generation. In: Bilezikian JP, Gaisz LG, Rodan GA (eds.) Principles of Bone Biology, vol. 1. Academic Press, San Diego, CA, USA, pp. 109–126.
9. Miyaura C, Onoe Y, Inada M, Maki K, Ikuta K, Ito M, Suda T 1997 Increased B-lymphopoiesis by interleukin 7 induces bone loss in mice with intact ovarian function: Similarity to estrogen deficiency. Proc Natl Acad Sci USA **94:**9360–9365.
10. Horowitz MC, Xi Y, Pflugh DL, Hesslein DG, Schatz DG, Lorenzo JA, Bothwell AL 2004 Pax5-deficient mice exhibit early onset osteopenia with increased osteoclast progenitors. J Immunol **173:**6583–6591.
11. Manabe N, Kawaguchi H, Chikuda H, Miyaura C, Inada M, Nagai R, Nabeshima Y, Nakamura K, Sinclair AM, Scheuermann RH, Kuro-o M 2001 Connection between B lymphocyte and osteoclast differentiation pathways. J Immunol **167:**2625–2631.
12. Sato T, Shibata T, Ikeda K, Watanabe K 2001 Generation of bone-resorbing osteoclasts from B220+ cells: Its role in accelerated osteoclastogenesis due to estrogen deficiency. J Bone Miner Res **16:**2215–2221.
13. Calvi LM, Adams GB, Weibrecht KW, Weber JM, Olson DP, Knight MC, Martin RP, Schipani E, Divieti P, Bringhurst FR, Milner LA, Kronenberg HM, Scadden DT 2003 Osteoblastic

cells regulate the haematopoietic stem cell niche. Nature **425:**841–846.
14. Taichman RS, Reilly MJ, Emerson SG 1996 Human osteoblasts support human hematopoietic progenitor cells in vitro bone marrow cultures. Blood **87:**518–524.
15. Zhu J, Garrett R, Jung Y, Zhang Y, Kim N, Wang J, Joe GJ, Hexner E, Choi Y, Taichman R, Emerson SG 2007 Osteoblasts support B lymphocyte commitment and differentiation from hematopoietic stem cells. Blood **109:**3706–3712.
16. Gohel A, McCarthy MB, Gronowicz G 1999 Estrogen prevents glucocorticoid-induced apoptosis in osteoblasts in vivo and in vitro. Endocrinology **140:**5339–5347.
17. Pantschenko AG, Zhang W, Nahounou M, McCarthy MB, Stover ML, Lichtler AC, Clark SH, Gronowicz GA 2005 Effect of osteoblast-targeted expression of bcl-2 in bone: Differential response in male and female mice. J Bone Miner Res **20:**1414–1429.
18. Bellido T, Ali AA, Plotkin LI, Fu Q, Gubrij I, Roberson PK, Weinstein RS, O'Brien CA, Manolagas SC, Jilka RL 2003 Proteasomal degradation of Runx2 shortens parathyroid hormone-induced anti-apoptotic signaling in osteoblasts. A putative explanation for why intermittent administration is needed for bone anabolism. J Biol Chem **278:**50259–50272.
19. Dobnig H, Turner RT 1997 The effects of programmed administration of human parathyroid hormone fragment (1-34) on bone histomorphometry and serum chemistry in rats. Endocrinology **138:**4607–4612.
20. Neer RM, Arnaud CD, Zanchetta JR, Prince R, Gaich GA, Reginster JY, Hodsman AB, Eriksen EF, Ish-Shalom S, Genant HK, Wang O, Mitlak BH 2001 Effect of parathyroid hormone (1-34) on fractures and bone mineral density in postmenopausal women with osteoporosis. N Engl J Med **344:**1434–1441.
21. Jilka RL, Weinstein RS, Bellido T, Roberson P, Parfitt AM, Manolagas SC 1999 Increased bone formation by prevention of osteoblast apoptosis with parathyroid hormone. J Clin Invest **104:**439–446.
22. Gubrij I, Ali AA, Chambers TM, Berryhill SB, Liu X, Roberson P, O'Brien CA, Weinstein RS, Manolagas SC, Jilka RL 2003 Decreased osteoblast apoptosis and increased bone formation in implants of marrow-derived osteoblast progenitors overexpressing bcl-2: In vivo evidence for a pivotal role of apoptosis in bone formation. J Bone Miner Res **18:**S1;S136.
23. Servet-Delprat C, Arnaud S, Jurdic P, Nataf S, Grasset MF, Soulas C, Domenget C, Destaing O, Rivollier A, Perret M, Dumontel C, Hanau D, Gilmore GL, Belin MF, Rabourdin-Combe C, Mouchiroud G 2002 Flt3+ macrophage precursors commit sequentially to osteoclasts, dendritic cells and microglia. BMC Immunol **3:**1–15.
24. Demiralp B, Chen HL, Koh AJ, Keller ET, McCauley LK 2002 Anabolic actions of parathyroid hormone during bone growth are dependent on c-fos. Endocrinology **143:**4038–4047.
25. Koh AJ, Demiralp B, Neiva KG, Hooten J, Nohutcu RM, Shim H, Datta NS, Taichman RS, McCauley LK 2005 Cells of the osteoclast lineage as mediators of the anabolic actions of parathyroid hormone in bone. Endocrinology **146:**4584–4596.
26. Berry JE, Ealba EL, Pettway GJ, Datta NS, Swanson EC, Somerman MJ, McCauley LK 2006 JunB as a Downstream Mediator of PTHrP Actions in Cementoblasts. J Bone Miner Res **21:**246–257.
27. Boot-Handford RP, Michaelidis TM, Hillarby MC, Zambelli A, Denton J, Hoyland JA, Freemont AJ, Grant ME, Wallis GA 1998 The bcl-2 knockout mouse exhibits marked changes in osteoblast phenotype and collagen deposition in bone as well as a mild growth plate phenotype. Int J Exp Pathol **79:**329–335.
28. Marks SC Jr, Seifert MF 1985 The lifespan of osteoclasts: Experimental studies using the giant granule cytoplasmic marker characteristic of beige mice. Bone **6:**451–455.
29. Fuller K, Owens JM, Jagger CJ, Wilson A, Moss R, Chambers TJ 1993 Macrophage colony-stimulating factor stimulates survival and chemotactic behavior in isolated osteoclasts. J Exp Med **178:**1733–1744.
30. Kurihara N, Chenu C, Miller M, Civin C, Roodman GD 1990 Identification of committed mononuclear precursors for osteoclast-like cells formed in long term human marrow cultures. Endocrinology **126:**2733–2741.
31. McGill GG, Horstmann M, Widlund HR, Du J, Motyckova G, Nishimura EK, Lin YL, Ramaswamy S, Avery W, Ding HF, Jordan SA, Jackson IJ, Korsmeyer SJ, Golub TR, Fisher DE 2002 Bcl2 regulation by the melanocyte master regulator Mitf modulates lineage survival and melanoma cell viability. Cell **109:**707–718.
32. Marchetti MC, Di Marco B, Cifone G, Migliorati G, Riccardi C 2003 Dexamethasone-induced apoptosis of thymocytes: Role of glucocorticoid receptor-associated Src kinase and caspase-8 activation. Blood **101:**585–593.
33. Lukert BP, Raisz LG 1990 Glucocorticoid-induced osteoporosis: Pathogenesis and management. Ann Intern Med **112:**352–364.
34. O'Brien CA, Jia D, Plotkin LI, Bellido T, Powers CC, Stewart SA, Manolagas SC, Weinstein RS 2004 Glucocorticoids act directly on osteoblasts and osteocytes to induce their apoptosis and reduce bone formation and strength. Endocrinology **145:**1835–1841.
35. Pagel CN, de Niese MR, Abraham LA, Chinni C, Song SJ, Pike RN, Mackie EJ 2003 Inhibition of osteoblast apoptosis by thrombin. Bone **33:**733–743.
36. Davies JH, Evans BA, Jenney ME, Gregory JW 2002 In vitro effects of chemotherapeutic agents on human osteoblast-like cells. Calcif Tissue Int **70:**408–415.
37. Chen HL, Demiralp B, Schneider A, Koh AJ, Silve C, Wang CY, McCauley LK 2002 Parathyroid hormone and parathyroid hormone-related protein exert both pro- and anti-apoptotic effects in mesenchymal cells. J Biol Chem **277:**19374–19381.
38. Lynch MP, Capparelli C, Stein JL, Stein GS, Lian JB 1998 Apoptosis during bone-like tissue development in vitro. J Cell Biochem **68:**31–49.
39. Stanislaus D, Yang X, Liang JD, Wolfe J, Cain RL, Onyia JE, Falla N, Marder P, Bidwell JP, Queener SW, Hock JM 2000 In vivo regulation of apoptosis in metaphyseal trabecular bone of young rats by synthetic human parathyroid hormone (1-34) fragment. Bone **27:**209–218.
40. Onyia JE, Bidwell J, Herring J, Hulman J, Hock JM 1995 In vivo, human parathyroid hormone fragment (hPTH 1-34) transiently stimulates immediate early response gene expression, but not proliferation, in trabecular bone cells of young rats. Bone **17:**479–484.
41. Lindsay R, Zhou H, Cosman F, Nieves J, Dempster DW, Hodsman AB 2007 Effects of a one-month treatment with PTH(1-34) on bone formation on cancellous, endocortical, and periosteal surfaces of the human ilium. J Bone Miner Res **22:**495–502.
42. Malluche H, Faugere MC 1990 Renal bone disease 1990: An unmet challenge for the nephrologist. Kidney Int **38:**193–211.
43. Sorenson CM, Rogers SA, Korsmeyer SJ, Hammerman MR 1995 Fulminant metanephric apoptosis and abnormal kidney development in bcl-2-deficient mice. Am J Physiol **268:**F73–F81.
44. Pettway GJ, Schneider A, Koh AJ, Widjaja E, Morris MD, Meganck JA, Goldstein SA, McCauley LK 2005 Anabolic actions of PTH (1-34): Use of a novel tissue engineering model to investigate temporal effects on bone. Bone **36:**959–970.

Address reprint requests to:
Laurie K McCauley, DDS, PhD
University of Michigan School of Dentistry
1011 N. University Avenue
Ann Arbor, MI 48109-1078, USA
E-mail: mccauley@umich.edu

Received in original form August 30, 2007; revised form November 13, 2007; accepted December 14, 2007.